A Novel, Evolutionarily Conserved Protein Phosphatase Complex Involved in Cisplatin Sensitivity*[S]

Anne-Claude Gingras‡§, Michael Caballero¶, Marcel Zarske¶, Amy Sanchez‡, Tony R. Hazbun‖, Stanley Fields‖, Nahum Sonenberg‡‡, Ernst Hafen¶, Brian Raught‡, and Ruedi Aebersold‡§§¶¶**

Using a combination of tandem affinity purification tagging and mass spectrometry, we characterized a novel, evolutionarily conserved protein phosphatase 4 (PP4)-containing complex (PP4cs, protein phosphatase 4, cisplatin-sensitive complex) that plays a critical role in the eukaryotic DNA damage response. PP4cs is comprised of the catalytic subunit PP4C; a known regulatory subunit, PP4R2; and a novel protein that we termed PP4R3. The *Saccharomyces cerevisiae* PP4R3 ortholog Psy2 was identified previously in a screen for sensitivity to the DNA-damaging agent and anticancer drug cisplatin. We demonstrated that deletion of any of the PP4cs complex orthologs in *S. cerevisiae* elicited cisplatin hypersensitivity. Furthermore human PP4R3 complemented the yeast *psy2* deletion, and *Drosophila melanogaster* lacking functional PP4R3 (*flfl*) exhibited cisplatin hypersensitivity, suggesting a highly conserved role for PP4cs in DNA damage repair. Finally we found that PP4R3 may target PP4cs to the DNA damage repair machinery at least in part via an interaction with Rad53 (CHK2). *Molecular & Cellular Proteomics 4:1725–1740, 2005.*

Reversible protein phosphorylation is a highly conserved, essential regulatory mechanism involved in a host of cellular processes. Yet, while the phosphorylation of regulatory molecules by kinases has been studied intensively, their subsequent dephosphorylation is much less well understood. In eukaryotes, dephosphorylation on serine/threonine residues is effected by two distinct groups of functionally diverse phosphatases, the phosphoprotein M (represented by a sole member in higher eukaryotes, PP2C) and PPP[1] families (1). Within the much larger PPP class, a common catalytic domain (of 280 aa) is highly conserved, whereas the N and C termini are more divergent and further separate the PPP proteins into subfamilies. A number of distinct PPP subfamilies have thus been characterized (PP1, PP2A, PP2B, PP5, and PP7; Ref. 2) based on sequence homology, associated regulatory subunits, sensitivity to different types of chemical inhibitors, and metal ion requirements. A major PPP subfamily that plays a variety of critical roles in a multitude of physiological processes is the PP2A-type phosphatases, PP2AC (the catalytic subunit of PP2A; human gene names *PPP2CA* and *PPP2CB*), PP4C (gene name *PPP4C*, formerly known as PPX), and PP6C (PPP6C; Ref. 3).

PP2A often functions as a standard trimeric complex with a catalytic (C) subunit (encoded by two genes in mammals) associated with one of many regulatory (or B) subunits via one of two adaptor (A) molecules (4, 5). The regulatory and adaptor subunits are thought to confer substrate specificity to the complex (5).

In contrast to PP2A, the supramolecular architecture and subunit composition of PP4 multiprotein complexes remains largely unknown. Two mammalian PP4 regulatory subunits were previously identified (here termed PP4R1 and PP4R2, gene names *PPP4R1* and *PPP4R2*; Refs. 6 and 7). Although PP4R1 shares some sequence homology with the PP2A adaptor proteins (*PPP2R1A* and *PPP2R1B*), it does not bridge PP4C and PP4R2; PP4R1 and PP4R2 display mutually exclusive PP4C interactions (Refs. 6 and 7; and see below). Other PP4C-interacting partners have also been reported (*e.g.* Refs. 8 and 9), but whether these proteins represent *bona fide* regulatory subunits or phosphatase substrates and how these binding proteins may affect PP4 activity are unclear.

To gain a better understanding of the composition, function, and regulation of PP4, we systematically analyzed mammalian and yeast PP4C-interacting proteins. In doing so, we

From the ‡Institute for Systems Biology, Seattle, Washington 98103, ¶Zoological Institute and ¶¶Faculty of Natural Science, University of Zurich, Zurich CH-8057, Switzerland, ‖Howard Hughes Medical Institute, Departments of Genome Sciences and Medicine, University of Washington, Seattle, Washington 98195, ‡‡Department of Biochemistry and McGill Cancer Centre, McGill University, Montréal, Quebec H3G 1Y6, Canada, and §§Institute for Molecular Systems Biology, ETH Hönggerberg, Zurich CH-8093, Switzerland

Received, July 26, 2005, and in revised form, August 2, 2005

Published, MCP Papers in Press, August 5, 2005, DOI 10.1074/mcp.M500231-MCP200

[1] The abbreviations used are: PPP, phosphoprotein phosphatase; TAP, tandem affinity purification; NTAP, N-terminal TAP; CTAP, C-terminal TAP; PP, protein phosphatase; PP4cs, protein phosphatase 4, cisplatin-sensitive; aa, amino acid(s); TEV, tobacco etch virus; HA, hemagglutinin; HEK, human embryonic kidney; HRP, horseradish peroxidase; Pol, polymerase; YPD, yeast-peptone-dextrose growth medium; MGC, mammalian gene collection.

This is an open access article under the CC BY license.

© 2005 by The American Society for Biochemistry and Molecular Biology, Inc.
This paper is available on line at http://www.mcponline.org

were able to characterize several different mutually exclusive PP4C-containing complexes and identified a novel, evolutionarily conserved PP4C binding partner (which we termed PP4R3) that assembles into a complex with PP4C and PP4R2. Interestingly deletion of the yeast PP4R3 ortholog *PSY2* was demonstrated previously to elicit hypersensitivity to the DNA damage-inducing drug cisplatin (10). We found that deletion of the other components of the yeast PP4C·PP4R2·PP4R3 complex also yielded cisplatin hypersensitivity; therefore we termed this complex PP4cs (protein phosphatase 4, cisplatin-sensitive; see below).

Platinum-based anticancer agents such as cisplatin and carboplatin display a broad range of activities against solid tumors (11, 12). However, the response to platinum-induced DNA damage is not well understood; multiple intracellular signaling pathways are clearly involved in DNA repair (12). A common problem with cisplatin-based cancer therapies is resistance to cisplatin. A better understanding of the cellular processes and effectors involved in the response to cisplatin treatment may thus improve our ability to treat cancer.

EXPERIMENTAL PROCEDURES

Plasmids and Yeast Strains—pcDNA3-flagA was a kind gift from Dr. S. Morino, and pcDNA3-GST and the original pcDNA3–3HA were generous gifts from Dr. H. Imataka. pESC-URA was purchased from Stratagene, and the yeast two-hybrid vectors were described previously (13, 14). The yeast tandem affinity purification (TAP) tag strains as well as diploid deletion strains in the BY4743 background and haploid MATα strains in the BY4742 background were from Open Biosystems. The yeast two-hybrid strains pJ69-4A and pJ69-4α as well as the vectors pOAD and pOBD-2 were described previously (13, 14).

To generate mammalian TAP tag vectors for the production of N-terminal (NTAP) and C-terminal (CTAP) fusion proteins, the TAP sequences (from the versions with two immunoglobulin binding domains, a TEV site, and a calmodulin binding domain) from the *Schizosaccharomyces pombe* vectors pREP-NTAP or pFA6a-2xPA-CTAP (Ref. 15; kind gifts from Dr. K. Gould, Vanderbilt University) were amplified by PCR. For NTAP, the 5′ primer introduced a KpnI site, whereas the 3′ primer introduced sites for PmeI, AscI, PacI, and BamHI. The PCR product was digested with KpnI and BamHI and inserted into the KpnI and BamHI sites of pcDNA3 (Invitrogen). For CTAP, the 5′ primer added an XhoI site followed by sites for PmeI, AscI, and PacI, whereas the 3′ primer introduced an ApaI site. The PCR product was digested with XhoI and ApaI and inserted into the XhoI and ApaI sites of pcDNA3. Inserts were completely sequenced. Unique sites and polylinker sequence for pcDNA3-NTAP and pcDNA3-CTAP are shown in Supplemental Fig. 1 and at www.proteomecenter.org.

To generate pcDNA3-flag$_{new}$ and pcDNA3-EE (Glu-Glu), adapters encoding the sequences MDYKDDDDKAAS and MEYMPMEAAS, respectively, were cloned into the KpnI and PmeI sites of pcDNA3-NTAP (thereby replacing the NTAP cassette with the appropriate epitope tag). pcDNA3–3HA$_{new}$ was generated by amplifying the triple HA tag from the original pcDNA3-3HA (a kind gift from Dr. H. Imataka) and inserting this tag into the KpnI/PmeI sites of pcDNA3-NTAP. All epitopes and multiple cloning site were sequenced.

Coding sequences for proteins of interest were amplified by PCR using *Pfu* Ultra from yeast genomic DNA (all yeast ORFs), a cDNA library from HeLa cells (Stratagene; hTIP41, NM_152902; PP2ACα, NM_002715; PP2ACβ, NM_004156; PP4C, NM_002720; PP6C, NM_002721), a cDNA library from human placenta (Ambion; PP4R2, NM_174907), a pcDNA3-alpha4 (alpha4) construct kindly provided by Dr. K. Arndt (NM_001551), or clones from the mammalian gene collection (MGC) or IMAGE clones (KIAA2010, NM_032560; KIAA1387, NM_020463; TCP1, NM_030752; PP1C, NM_002708). All accession numbers in parentheses are from GenBank™. Inserts were cloned in-frame into appropriate vectors. 3′ and 5′ junctions of all inserts or entire inserts obtained through library amplification were sequenced.

Preparation of Extracts and Detection of Expression Levels—For stable cell pools, low passage number HEK293 cells (ATCC; CRL-1573) were transfected with Lipofectamine PLUS (Invitrogen) according to the manufacturer's instructions and selected with 750 μg/ml active G418 (Mediatech cellgro). Selection medium was changed every 2–3 days for ~14 days when a stable cell population was obtained. Expression was monitored, and cells were amplified further to generate ~10–20 150-mm plates per experiment.

Cells were washed three times in ice-cold PBS, harvested by scraping, and then centrifuged to remove excess PBS. TAP lysis buffer (10% glycerol, 50 mM Hepes-KOH, pH 8.0, 100 mM KCl, 2 mM EDTA, 0.1% Nonidet P-40, 2 mM DTT, 10 mM NaF, 0.25 mM $NaOVO_3$, and 50 mM β-glycerophosphate supplemented with 1× protease inhibitor mixture (Sigma catalog number P8340), 5 nM okadaic acid, and 5 nM calyculin A) was added (0.5–1 ml of lysis buffer/150-mm plate), and the mixture was incubated on ice for 30 min. Lysis was further enhanced by performing two freeze-thaw cycles. In preliminary experiments, varying concentrations of the specific serine/threonine phosphatase inhibitors were used; the interactions reported here were observed under all conditions.

Saccharomyces cerevisiae TAP tag strains (Open Biosystems) were grown to OD 0.8–1.0 and harvested by centrifugation. After one rinsing step in 20 mM Hepes, pH 7.5, 10 mM EDTA, cells were pelleted and flash frozen. Pellets were thawed in TAP lysis buffer using 1 ml of lysis buffer/g. Yeast were lysed by glass bead beating.

For the preparation of cleared extract from mammalian cells or yeast, debris were pelleted via centrifugation (15,000 rpm for 30 min at 4 °C), and protein concentration was determined by a Bradford-type assay (Bio-Rad). Expression levels of recombinant proteins in transfected mammalian cells or yeast strains were analyzed by separating 10–25 μg of total cell extract by SDS-PAGE followed by immunoblotting with normal rabbit serum (ICN Biomedicals Inc.; 1:2000) as the primary antibody and donkey anti-rabbit-horseradish peroxidase (HRP) (Amersham Biosciences; 1:5000) as a secondary antibody.

TAP Tag Purification—The purification strategy used here was largely the same as that described by Rigaut *et al.* (16) with minor modifications (see below) and adaptation for direct LC-MS analysis. More details may be found at www.proteomecenter.org.

Mammalian cells or yeast were lysed in TAP lysis buffer, and extracts were centrifuged to remove debris as described above. Mammalian TAP tag purifications were performed with extract from 5–20 15-cm plates of stably transfected HEK293 cells (roughly 40–150 mg of protein extract). Alternatively TAP purification was performed with extract from 1–2 liters of yeast grown to OD 0.8–1.0. Extracts were incubated with 100 μl of packed, prewashed IgG-Sepharose beads (Amersham Biosciences) for 4–6 h at 4 °C with gentle agitation. Beads were pelleted and washed three times with TAP lysis buffer and three times with TEV cleavage buffer (10 mM Hepes-KOH, pH 8.0, 150 mM NaCl, 0.1% Nonidet P-40, 0.5 mM EDTA, and 1 mM DTT). Beads were then resuspended in 300 μl of TEV lysis buffer containing 100–200 units of recombinant AcTEV (Invitrogen) and returned to incubation with gentle agitation at 4 °C for 10–16 h. After TEV cleavage, the IgG beads were pelleted, and the super-

natant was transferred to a fresh tube. IgG beads were rinsed three times with calmodulin binding buffer (10 mM Hepes-KOH, pH 8.0, 150 mM NaCl, 10 mM β-mercaptoethanol, 1 mM MgOAc, 1 mM imidazole, 0.1% Nonidet P-40, and 2 mM $CaCl_2$), and all washes were combined with the supernatant. $CaCl_2$ (5 μl of a 1 M stock) was added to the mixture, which was centrifuged once more and then transferred to a fresh tube containing 75 μl of packed calmodulin-Sepharose beads (Amersham Biosciences). Incubation was performed for 2–3 h at 4 °C with agitation. The slurry was transferred into empty Bio-spin columns (Bio-Rad), and the flow-through was removed through gentle air pressure. Two washes in calmodulin binding buffer (750 μl each) were performed followed by three washes in calmodulin rinsing buffer (50 mM ammonium bicarbonate, pH 8.3, 75 mM NaCl, 1 mM MgOAc, 1 mM imidazole, and 2 mM $CaCl_2$). The last drops of rinsing buffer were drained with gentle pressure, and Bio-spin columns were transferred to fresh tubes. Two elutions with 100 μl each of calmodulin elution buffer (50 mM ammonium bicarbonate, pH 8.3, and 25 mM EGTA, pH 8.0) were performed, and the Bio-spin column was transferred into another tube for two additional elutions.

Trypsin Digest and Preparation for Mass Spectrometry—Sequencing grade modified trypsin (Promega; 0.5–1 μg) was added directly to the eluate. Digestion was performed overnight at 37 °C. Following digestion, the sample was lyophilized and then resuspended in reversed-phase HPLC buffer A (20 μl; 0.4% AcOH, 0.005% heptafluorobutyric anhydride in H_2O). Prior to loading onto the reversed-phase column, the sample was centrifuged at 13,000 rpm for 10 min, and the supernatant was transferred to a fresh tube.

LC-MS/MS—Microcapillary reversed-phase columns (75-μm inner diameter, 363-μm outer diameter; Polymicro Technology) were cut to a final length of 15–20 cm, and spray tips were pulled in-house by hand. Columns were packed in-house (12 cm) with Magic C_{18} 100-Å, 5-μm silica particles (Michrom, catalog number PM5/61100/00) using a pressure bomb. Prior to loading the sample, columns were equilibrated in HPLC buffer A. Half of the sample was applied to the column using a pressure bomb and then washed off line in buffer A + 5% acetonitrile for 30–60 min. The LC column was then placed in front of a Finnigan LCQ mass spectrometer, programmed for data-dependent MS/MS acquisition (one survey scan, three MS/MS of the most abundant ions). After sequencing the same species three times, the mass ± 3 Da was placed on an exclusion list for 3 min. Peptides were eluted from the reversed-phase column using a multiphasic elution gradient (5–14% acetonitrile over 5 min, 14–40% over 60 min, and 40–80% over 10 min). The remaining half of the sample was then processed in the same manner. To prevent cross-contamination, each sample was processed on a freshly prepared reversed-phase column.

Data Analysis—Raw files generated by Xcalibur (Finnigan) were converted to the mzXML format (17), and combined runs (from the same sample) were searched using SEQUEST against the human International Protein Index (IPI) database, version 3.01, or against the *Saccharomyces* Genome Database (SGD) yeast ORF database (April 22, 2004 version). SEQUEST searches were performed without constraining for the number of tryptic termini, with a mass tolerance on the precursor ion of ±2, and methionine oxidation (+16) as a variable modification. SEQUEST html output was analyzed with INTERACT (18), PeptideProphet (19), and ProteinProphet (20) using the default parameters of each program. With the exception of Xcalibur and SEQUEST, all other software tools are open source and available from the Institute for Systems Biology (www.proteomecenter.org/software.php).

Non-radioactive Transcription/Translation Assays—Mixtures of plasmid DNA containing a T7 promoter (100–500 ng) were used to program 25 μl of a reticulocyte transcription/translation system containing Transcend tRNA (Promega) essentially according to the manufacturer's instructions. Translated proteins were subjected to SDS-PAGE and transferred to a nitrocellulose membrane. The membrane was blocked for 1 h in PBS + 0.5% Tween 20. Streptavidin-HRP (Amersham Biosciences; 1:10,000) was used to detect the newly synthesized proteins incorporating biotinylated lysine. After washing the membrane (3 × 5 min with PBS + 0.5% Tween 20; 3 × 5 min with water), chemiluminescence was performed. Immunoprecipitations were performed by diluting the TNT reaction with TAP lysis buffer and incubating with 5–10 μl of packed anti-HA beads (Roche Applied Science) or anti-FLAG resin (Sigma). After three washes with TAP lysis buffer, the sample was eluted directly in protein sample buffer lacking reducing agent by incubation for 30 min at 37 °C. Reducing agent was added, and the sample was boiled and loaded onto SDS-PAGE gels.

Cisplatin Sensitivity Assay in Drosophila—*flfl*^{2} (I57T) and *flfl*^{3} (premature stop codon at position 347) are ethyl methanesulfonate-induced alleles. Healthy heterozygous flies carrying either *flfl*^{2} or *flfl*^{3} over a marker chromosome (MKRS) were maintained on apple agar plates at 25 °C and allowed to lay eggs for 24 h. Agar plates were then changed and incubated for another 24 h at 25 °C. First instar larvae were collected and distributed to vials containing standard fly food into which the cisplatin solution was allowed to diffuse. Cisplatin powder (Alexis Biochemicals, Lausanne, Switzerland) was dissolved in 0.9% NaCl to obtain 0.4, 0.8, and 1.2 mM stock solutions. To test for putative undesirable effects of the MKRS marker chromosome, MKRS/+ flies were also tested for cisplatin sensitivity. The MKRS/+ as well as the control *flfl*^{2}/+ or *flfl*^{3}/+ flies showed no change in cisplatin sensitivity as compared with wild type flies.

RESULTS

Identification of Human PP4C-binding Proteins—TAP tagging and mass spectrometry, in which a protein complex of interest is purified in a two-step affinity enrichment process and its components are identified by the fragment ion spectra of selected tryptic peptides, have proven to be invaluable tools in the characterization of protein complexes (16, 21–23). As compared with single tag purification strategies, samples isolated by TAP tagging are significantly cleaner, thereby reducing the likelihood of false-positive identifications. Harsh washing conditions are also not necessary, allowing for recovery of native complexes. Another advantage of such approaches is that they are generic, making them particularly suited to the study of interaction networks in which binding partners for multiple proteins can be analyzed in parallel.

To gain insight into the supramolecular architecture of PP4-containing complexes, we tagged the catalytic subunit at its N terminus with a TAP tag, expressed this protein stably in HEK293 cells, and then processed the tagged protein along with its binding partners for purification (see "Experimental Procedures" and Fig. 1*A*). Eluted proteins were subjected to LC-MS/MS and identified via database searching followed by statistical analysis of the search results using a suite of software tools, including PeptideProphet and ProteinProphet (Refs. 19 and 20; see "Experimental Procedures"). To establish a list of background contaminant proteins, we analyzed cells stably expressing the TAP tag alone. In addition, proteins detected in numerous unrelated samples were flagged as dubious interactors and added to the contaminant list (see Supplemental Table I). For a list of PP4C-interacting pro-

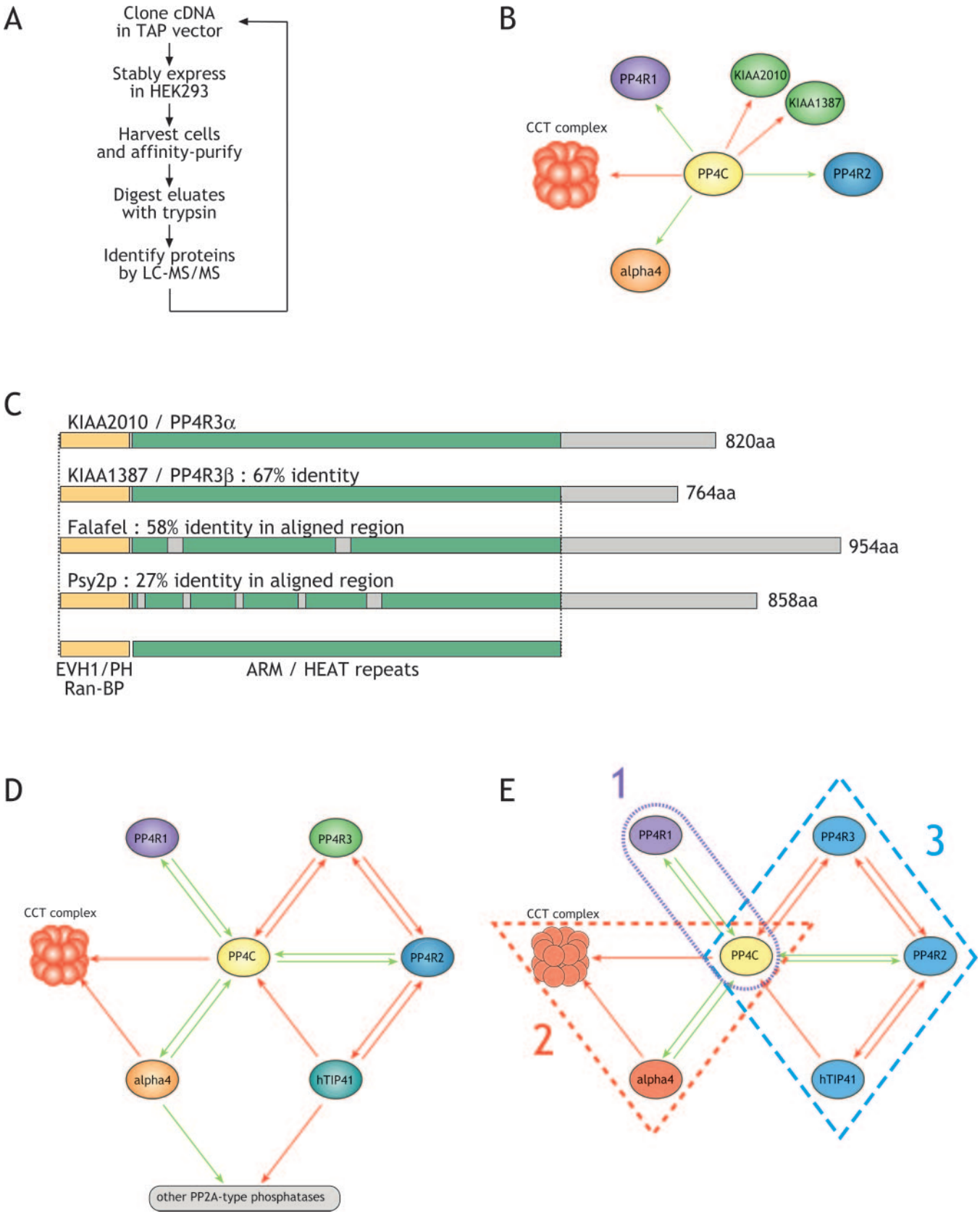
A
Clone cDNA in TAP vector
Stably express in HEK293
Harvest cells and affinity-purify
Digest eluates with trypsin
Identify proteins by LC-MS/MS
B
PP4R1
KIAA2010
KIAA1387
CCT complex
PP4C
PP4R2
alpha4
C
KIAA2010 / PP4R3α
820aa
KIAA1387 / PP4R3β : 67% identity
764aa
Falafel : 58% identity in aligned region
954aa
Psy2p : 27% identity in aligned region
858aa
EVH1/PH Ran-BP
ARM / HEAT repeats
D
PP4R1
PP4R3
CCT complex
PP4C
PP4R2
alpha4
hTIP41
other PP2A-type phosphatases
E
1
2
3
PP4R1
PP4R3
CCT complex
PP4C
PP4R2
alpha4
hTIP41

TABLE I
Human protein interactions detected by mass spectrometry

		Statistical data for interacting partners					
Tagged protein	Interactors	Accession	Protein Prophet p value	Unique peptides	Total peptides	Percent protein coverage	Coverage ratio
PP4C	IGBP1	NP_001542	1.00	10	16	33.6	0.85
	PP4R1	NP_005125	1.00	3	8	5.7	0.14
	PP4R2	NP_777567	1.00	11	20	42.2	1.07
	TCP1	NP_110379	1.00	13	24	29.8	0.76
	CCT2	NP_006422	1.00	15	22	34.4	0.87
	CCT3	NP_005989	1.00	5	11	14.9	0.38
	CCT4	NP_006421	1.00	7	15	22.2	0.56
	CCT5	NP_036205	1.00	15	30	35.5	0.90
	CCT6A	NP_001753	1.00	9	18	22.6	0.57
	CCT7	NP_006420	1.00	14	29	31.7	0.80
	CCT8	NP_006576	1.00	17	22	29.8	0.76
	KIAA2010/ PP4R3α	NP_115949	1.00	11	19	20.0	0.51
	KIAA1387/ PP4R3β	NP_065196	1.00	3	3	5.6	0.14
PP4R1	PP4C	NP_002711	1.00	14	31	40.1	1.70
IGBP1	TCP1	NP_110379	1.00	20	49	45.1	0.62
	CCT2	NP_006422	1.00	25	54	44.5	0.62
	CCT3	NP_005989	1.00	19	35	30.7	0.42
	CCT4	NP_006421	1.00	14	41	29.2	0.40
	CCT5	NP_036205	1.00	25	46	36.4	0.50
	CCT6A	NP_001753	1.00	19	42	35.2	0.49
	CCT7	NP_006420	1.00	17	32	35.4	0.49
	CCT8	NP_006576	1.00	24	50	39.6	0.55
	PP4C	NP_002711	1.00	1	1	6.2	0.09
	PP6C	NP_002712	0.98	1	2	6.2	0.09
	PP2AC	NP_002706	1.00	3	11	8.4	0.12
TCP1	CCT2	NP_006422	1.00	24	56	50.7	1.00
	CCT3	NP_005989	1.00	17	34	26.8	0.53
	CCT4	NP_006421	1.00	14	26	31.2	0.61
	CCT5	NP_036205	1.00	18	47	41.8	0.82
	CCT6A	NP_001753	1.00	17	39	35.2	0.69
	CCT7	NP_006420	1.00	18	39	31.7	0.62
	CCT8	NP_006576	1.00	19	25	29.6	0.58
PP4R2	PP4C	NP_002711	1.00	13	41	25.4	0.38
	KIAA2010/ PP4R3α	NP_115949	1.00	36	98	44.3	0.66
	KIAA1387/ PP4R3β	NP_065196	1.00	12	24	17.0	0.25
	MGC3794/ hTIP41	NP_690866	1.00	3	3	23.2	0.45
hTIP41	PP4C	NP_002711	0.94	1	1	6.5	0.13
	PP4R2	NP_777567	1.00	3	7	15.1	0.30
PP4R3α	PP4C	NP_002711	1.00	4	6	24.4	0.63
	PP4R2	NP_777567	1.00	16	28	49.6	1.28

teins see Table I. The data are also represented pictorially in Fig. 1*B*.

In addition to the recovery of the TAP-tagged "bait" protein itself (PP4C), we observed a number of peptides derived from the known PP4C regulatory subunits PP4R1 and PP4R2 (Table I). We also observed many peptides derived from alpha4 (*IGBP1*) previously demonstrated to interact directly with all of the PP2A-like phosphatase catalytic subunits (24, 25). Alpha4 is the ortholog of the yeast Tap42 protein, which links the target of rapamycin signaling pathway to PP2A-type phosphatases (26–28). However, the role of the PP2A-type phosphatases in rapamycin-sensitive signaling in mammals is not well understood.

Interestingly our analysis also identified all eight subunits of

FIG. 1. **Protein-protein interactions surrounding the mammalian PP4 catalytic subunit and identification of novel PP4C-interacting partners.** *A*, iterative TAP tag strategy to detect interacting proteins. *B*, proteins present in the TAP tag purification of the PP4 catalytic subunit. Only interactions detected in our TAP tag experiments are represented. *Green arrows* represent interactions that were also previously reported, whereas *red arrows* indicate novel interactions. *C*, PP4R3 is conserved throughout eukaryotic evolution. Shown is the alignment between KIAA2010, KIAA1387, Falafel, and Psy2p. *Green boxes* represent armadillo (*ARM*)/HEAT repeats, and the *yellow box* indicates a domain with homology to the Ran binding domain of RanBP1 as well as moderate homology with pleckstrin homology (*PH*) and EVH1 domains. *D*, PP4C interaction network. *Arrows* indicate directionality; bait → prey. hTIP41 and alpha4 were also found to be associated with the PP2A and PP6 phosphatases. *E*, PP4C appears to be a component of several different types of mutually exclusive complexes.

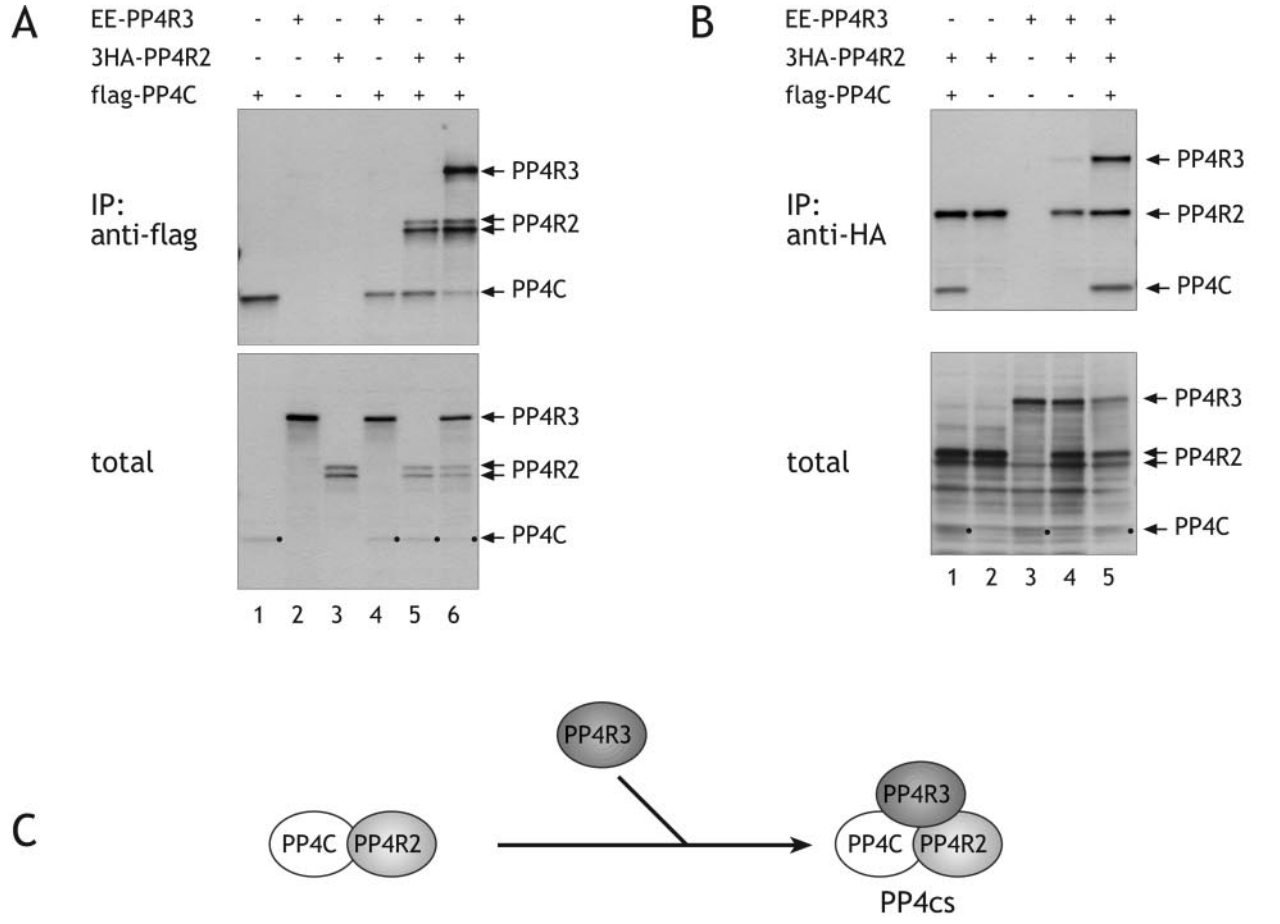
A
EE-PP4R3
3HA-PP4R2
flag-PP4C
IP:
anti-flag
PP4R3
PP4R2
PP4C
total
PP4R3
PP4R2
PP4C
1 2 3 4 5 6
B
EE-PP4R3
3HA-PP4R2
flag-PP4C
IP:
anti-HA
PP4R3
PP4R2
PP4C
total
PP4R3
PP4R2
PP4C
1 2 3 4 5
C
PP4C
PP4R2
PP4R3
PP4C
PP4R2
PP4R3
PP4cs
D
PP4R2 alone
PP4R2
PP4R3
flag-tagged
protein
PP2ACα
PP2ACβ
PP4C
PP6C
PP2ACα
PP2ACβ
PP4C
PP6C
IP:
anti-flag
PP4R3
PP4R2
catalytic
subunits
total
PP4R3
PP4R2
catalytic
subunits
1 2 3 4 5 6 7 8
E
GST-hTIP41
flag-tagged
protein
PP1C
PP2ACβ
PP4C
PP6C
alpha4
none
IP:
anti-flag
hTIP41
alpha4
catalytic
subunits
total
hTIP41
alpha4
catalytic
subunits
1 2 3 4 5 6

an ATP-dependent chaperonin, the TRiC/CCT complex. The TRiC/CCT complex was initially thought to be highly specialized for the folding and assembly of actin and tubulin, but recent work suggests that it participates in the folding and assembly of a broader range of substrates (23). The interaction with TRiC/CCT appears to be evolutionarily conserved as both Pph3 (the ortholog of PP4C) and Tap42 also co-precipitated with this complex in a large scale study (29). The functional significance of the TRiC/CCT complex interaction with PP4cat is unknown at this time.

A Novel Evolutionarily Conserved Protein Interacts with PP4C—Other than the known PP4C-interacting partners and the TRiC/CCT complex, only two additional (non-contaminant) proteins were detected in the TAP-PP4C purification: KIAA2010 and KIAA1387. The human KIAA2010 is 820 aa in length, and KIAA1387 is 764 aa. The two proteins share 67% sequence identity and 77% homology at the amino acid level (Fig. 1*C*). To be consistent with the nomenclature of the PP2A-type phosphatases, here we refer to KIAA2010 as PP4R3α and to KIAA1387 as PP4R3β (see below for further justification). PP4R3-like proteins are conserved throughout Eukaryotae: the *Drosophila* falafel (*flfl*) protein shares 58% identity with KIAA2010 at the amino acid level, and the *S. cerevisiae* Psy2 protein exhibits 27% identity with KIAA2010 over 699 amino acids (Fig. 1*C*).

The predicted two- and three-dimensional structure of the PP4R3 protein family indicates that a 115-aa fragment at the extreme N terminus shares extensive structural homology with a Ran binding domain found in RanBP1 (Fig. 1*C*). The predicted structure of this fragment is also reminiscent of pleckstrin homology domains. The Ran binding-like region is the most conserved portion of the protein across species, sharing 46% identity (60% similarity) at the amino acid level with yeast Psy2p and 87% identity (95% similarity) with *flfl*. Threading algorithms (30) indicate that the KIAA2010 and KIAA1387 proteins also possess a number of HEAT or armadillo repeats. Whether PP4R3 can interact with Ran is unknown at this time; we were unable to detect this interaction by co-immunoprecipitation following *in vitro* translation or co-transfection in 293 cells (data not shown).

Interestingly small interfering RNAs directed against KIAA1387 shorten mitotic transit time (31). Falafel (*flfl*) was first identified in a modular misexpression screen designed to identify novel dRac-specific signaling components; loss of *flfl* resulted in defects in dorsal closure, a phenomenon also associated with dRac deletion (Ref. 32; see below). Finally the yeast PP4R3 homolog was dubbed Psy2p based on hypersensitivity of deletants to the anticancer drug cisplatin (Ref. 10; see below).

Mammalian PP4 Module Interaction Network—To confirm the observed novel interactions and to better understand the supramolecular architecture of PP4C-containing complexes in mammals, we cloned the human alpha4, PP4R1 (*PPP4R1*), PP4R2 (*PPP4R2*), and PP4R3α (*KIAA2010*) ORFs into TAP tag vectors, established HEK293 cell lines stably expressing these tagged proteins, and repeated the purification and mass spectrometric identification process for each of these proteins and their interacting partners (Fig. 1, *A* and *D*, and Table I).

The PP4R1 pull-down yielded only the bait itself and PP4C. No peptides derived from alpha4, the TRiC/CCT complex, PP4reg2, or PP4reg3 were detected in these experiments (Table I). Alpha4 pull-downs yielded primarily TRiC/CCT complex proteins in addition to a single PP4C peptide and a few peptides from the other known alpha4 binding partners (PP6C, one peptide; and PP2AC, three peptides). In a PP4R2 pull-down, the TAP-tagged protein itself and PP4C were identified as well as many peptides from PP4R3α and PP4R3β. Thus, as with PP4C, PP4R2 appeared to be present in a complex with PP4R3α and/or PP4R3β. In addition to these proteins, the PP4R2 pull-down also yielded MGC3794, the human homolog of *S. cerevisiae* Tip41 (Tap42-interacting protein, molecular mass of 42 kDa), a protein involved in rapamycin signaling through phosphatase regulation (33, 34). We cloned the MGC3794 ORF (hereafter referred to as hTIP41) into the TAP tag vectors and repeated the pull-down/identification process with this fusion protein. PP4C and PP4R2 peptides (in addition to other phosphatase subunits, which will be reported elsewhere) were identified. This observation is intriguing because the yeast Tip41 protein was reported to interact with the yeast alpha4 homolog Tap42 and to prevent Tap42 from forming complexes with phosphatases (Ref. 33; see "Discussion"). Finally a pull-down of PP4R3α (KIAA2010) confirmed the interaction with PP4C and PP4R2. No additional proteins were identified in the PP4R3 pull-down.

Taken together, these data suggest that PP4C is present in several distinct complexes: 1) a binary complex with PP4R1, 2) a complex involving alpha4 and the chaperonin TRiC/CCT,

FIG. 2. **Assembly and specificity of the PP4C·PP4R2·PP4R3 complex.** *A* and *B*, epitope-tagged versions of PP4R3 (EE tag), PP4R2 (3HA tag), and PP4C (FLAG tag) were co-translated in a reticulocyte lysate containing biotinylated lysine ($\pm$ denotes addition of the corresponding cDNA to the reaction). Following co-translation, reactions were either analyzed directly by SDS-PAGE (*bottom panels*) or incubated with an anti-FLAG Sepharose resin (*A*) or anti-HA Sepharose resin (*B*) prior to gel analysis. Proteins were transferred to nitrocellulose and visualized by incubation with streptavidin-HRP followed by chemiluminescence. *Black dots* denote the location of the weaker PP4C band. *C*, model depicting the preassembly of a binary complex between PP4C and PP4R2 prior to the stable association of PP4R3 into PP4cs. *D* and *E*, specific interactions of PP4R2 and PP4R3 (but not hTIP41) with PP4C. PP4R2 (3HA-tagged; *D*), PP4R2 + PP4R3 (EE-tagged; *D*), or hTIP41 (GST-tagged; *E*) were co-translated in a reticulocyte lysate with the indicated FLAG-tagged catalytic subunit. Following translation, samples were analyzed directly via SDS-PAGE (*bottom panels*) or immunoprecipitated as above using an anti-FLAG Sepharose resin (*top panels*). *IP*, immunoprecipitation.

and 3) a complex containing PP4R2 and PP4R3, which may also include hTIP41 (Fig. 1*E*). The PP4C·PP4R2·PP4R3 complex will be referred to throughout this study as PP4cs (see below). These results also demonstrate how an iterative TAP tagging/mass spectrometry approach may be used to characterize the components of individual multiprotein complexes.

Interaction of PP4R3 with PP4C Requires Preassembly of PP4C and PP4R2—We next confirmed that PP4C, PP4R2, and PP4R3α (KIAA2010) form a multimeric complex. Each protein was tagged at its N terminus with a different epitope tag to allow for detection and immunoprecipitation. Plasmid DNA coding for each of the tagged proteins was used to program a coupled transcription/translation (TNT) reticulocyte lysate containing biotinylated lysine (see "Experimental Procedures"). Following separation by SDS-PAGE and transfer to a nitrocellulose membrane, translation products were detected using streptavidin conjugated to HRP. When all three proteins were co-translated, both 3HA-tagged PP4R2 and Glu-Glu (EE)-tagged PP4R3 were co-immunoprecipitated with FLAG-tagged PP4C (Fig. 2A, *lane 6*). (The 3HA-PP4R2 constructs often yielded two products with slightly different electrophoretic mobilities. This is most likely because of alternative translation initiation start site usage, since the smaller product does not react with the anti-HA antibody.) Similarly a 3HA-PP4R2 protein pull-down (Fig. 2*B*, *lane 5*) co-precipitated both FLAG-PP4C and EE-PP4R3. Exclusion of PP4R3 from the TNT reaction had no apparent effect on the interaction between FLAG-PP4C and 3HA-PP4R2 (Fig. 2*A*, *lane 5*). Thus, binary complex formation between FLAG-PP4C and 3HA-PP4R2 is not dependent on PP4R3. Importantly, however, omission of 3HA-PP4R2 from the TNT mixture precluded co-immunoprecipitation of EE-PP4R3 with FLAG-PP4C (Fig. 2*A*, *lane 4*), suggesting that PP4R2 is necessary to mediate the interaction between PP4C and PP4R3. Consistent with this observation, a two-hybrid association between the putative yeast orthologs of PP4R2 (Ybl046w) and PP4R3 (Psy2p; Ynl201c) was reported previously in a large scale study (Ref. 35; also see below). However, a putative direct interaction between PP4R2 and PP4R3 in the TNT system is apparently not sufficient for the formation of a stable complex as omission of FLAG-PP4C from the TNT mixture prevented efficient co-precipitation of EE-PP4R3 with 3HA-PP4R2 (Fig. 2*B*, compare *lanes 4* and *5*). It thus appears that a binary complex between PP4C and PP4R2 must be assembled before PP4R3 can stably interact as illustrated in Fig. 2*C*. This situation differs from the assembly of PP2AC-containing trimeric complexes in that the adapter (A subunit, or *PPP2R1*) can efficiently co-precipitate either the catalytic or the regulatory B subunits (*e.g.* Ref. 36).

PP4R2 and PP4R3 Interact with PP4C but Not with the Related Phosphatases PP2AC or PP6C—Our TAP tagging data strongly suggested that the binding of PP4R3 and PP4R2 is specific to PP4C: no peptides derived from other phosphatases were recovered following TAP-mediated purification of PP4R2 or PP4R3. Similarly no PP4R2 or PP4R3 (KIAA2010 or KIAA1387) peptides were observed following TAP-mediated purification of PP2AC, PP6C, or PP1C (data not shown). To confirm these observations, we tested whether the two regulatory proteins can co-precipitate with the other mammalian PP2A-type phosphatases. The coding sequences for PP2ACα (*PPP2CA*), PP2ACβ (*PPP2CB*), and PP6C (*PPP6C*) were cloned into the pcDNA3-flag vector and co-translated in a TNT lysate with 3HA-PP4R2 alone (Fig. 2*D*, *lanes 1–4*) or 3HA-PP4R2 and EE-PP4R3 (*lanes 5–8*). All catalytic subunits were expressed (*bottom panel*), yet PP4R2 and PP4R3 were only co-precipitated on an anti-FLAG Sepharose resin when co-expressed with FLAG-PP4C (*lanes 3* and *7*). The interaction with PP4C is thus specific, and PP4R3 (KIAA2010) appears to be a *bona fide* PP4 regulatory subunit.

The specificity of the PP4cs intracomplex interactions contrasts with that of hTIP41, which interacted with all of the PP2A-like phosphatase catalytic subunits in our study. Consistent with this, GST-hTIP41 co-translated with the FLAG-tagged phosphatases in the TNT system was efficiently co-immunoprecipitated with FLAG-PP2ACβ, FLAG-PP4C, and FLAG-PP6C (Fig. 2*E*, *lanes 2–4*). However, the serine/threonine phosphatase PP1C (the PPP phosphatase most closely related to PP2A with 41% identity to PP2AC) was unable to precipitate hTIP41 (*lane 1*). In this respect, hTIP41 resembles the human alpha4 protein, which can establish interactions with all PP2A-type phosphatases (24). In contrast to a previous report documenting an interaction between the *S. cerevisiae* Tip41 and Tap42 proteins (33), hTIP41 was unable to co-precipitate FLAG-alpha4 (Fig. 2*E*, *lane 5*). Taken together, these results indicate that hTIP41 can interact with all of the PP2A-type phosphatase catalytic subunits and is therefore not a specific interacting partner for the PP4 complex.

Interaction among Yeast Orthologs of the PP4 Complex—The *S. cerevisiae* genome contains orthologs of the mammalian PP4C, PP4R2, and PP4R3 proteins. The protein sharing the most homology to PP4R3 in *S. cerevisiae* is Psy2 (Ynl201c; Fig. 1*C*). The yeast Pph3 protein (Ydr075w) is most closely related to PP4C, although the sequences of the other *S. cerevisiae* PP2A-type phosphatases (Sit4, Pph21, Pph22, and Ppg1) are also closely related. Although no yeast protein exhibits sequence homology to PP4R2 throughout its entire sequence, the Ybl046w ORF possesses a small stretch of homology in its N terminus. Large scale experiments have provided evidence for interactions between these yeast orthologs; a two-hybrid interaction was reported between Psy2 and Ybl046w (35), and complexes containing Pph3, Ybl046w, and Psy2 (along with other proteins) have been detected using pull-down/mass spectrometry approaches (29, 37). We thus set out to determine whether yeast Pph3-containing complexes were organized in a manner similar to mammalian PP4C-containing complexes and whether a PP4cs-like complex has been conserved throughout evolution. To this end, we obtained yeast strains expressing C-terminally TAP-

TABLE II
Yeast protein interactions detected by mass spectrometry

		Statistical data for interacting partners					
Tagged protein	Interactors	ORF name	Protein Prophet p value	Unique peptides	Total peptides	Percent protein coverage	Coverage ratio
Pph3	Ybl046w	YBL046w	1.00	42	133	53.1	1.29
	Psy2	YNL201c	1.00	63	241	61.2	1.49
	Spt5	YML010w	1.00	12	17	16.3	0.40
Ybl046w	Pph3	YDR075w	1.00	18	59	32.8	0.46
	Psy2	YNL201c	1.00	74	228	71.2	1.00
	Spt4	YGR063w	0.92	1	2	10.8	0.15
	Spt5	YML010w	1.00	33	62	36.3	0.51
Tip41	Ybl046w	YBL046w	0.98	1	3	3.4	0.05
	Psy2	YNL201c	1.00	4	5	7.1	0.10
Psy2	Pph3	YDR075w	1.00	21	45	52.3	0.77
	Ybl046w	YBL046w	1.00	44	147	66.7	0.99
	Tip41	YPR040w	1.00	2	4	11.2	0.17
	Spt4	YGR063c	1.00	2	4	25.5	0.38
	Spt5	YML010w	1.00	28	57	32.9	0.49
Spt5	Spt4	YGR063c	1.00	7	32	45.1	0.80
	Ybl046w	YBL046w	1.00	4	9	15.4	0.27
	Psy2	YNL201c	1.00	5	10	10.5	0.19
	Rpb2	YOR151c	1.00	8	8	8.1	0.14
	Rpb3	YIL021w	1.00	3	5	10.7	0.19
	Rpb4	YJL140w	1.00	2	2	11.8	0.21

tagged Pph3, Ybl046w, Psy2, and Tip41 proteins and used the same purification and mass spectrometry approach to identify interacting partners for these polypeptides. As shown in Table II and Fig. 3, interactions among the yeast proteins were extremely similar to those we observed for the human PP4cs proteins: Pph3, Ybl046w, and Psy2 all established reciprocal interactions. As in the mammalian system, Tip41p was also associated with this complex, although the coverage ratio suggests that it was present in lower amounts than the other components. We did not detect the TRiC/CCT complex or alpha4 in the Pph3-TAP pull-down; however, this may be due to the presence of the relatively large TAP tag at the C terminus of the protein (the mammalian PP4C was tagged at its N terminus) as both Pph3-FLAG and Tap42-FLAG were previously shown to co-precipitate with the TRiC/CCT complex (29).

Interestingly, we also detected the transcription elongation factor complex components Spt4 and Spt5 in TAP tag purifications of both Psy2 and Ybl046w (Spt5 was also detected previously as a Psy2 and Ybl046w interactor in a large scale experiment; Ref. 37). Conversely purification of TAP-tagged Spt5 yielded Spt4 and RNA Pol II subunits, as expected, in addition to several peptides for Psy2, Ybl046w, and Pph3. A putative role for PP4cs may thus be to target the Pph3 phosphatase to the transcription elongation machinery.

The Yeast PP4cs Complex Is Involved in the Response to Cisplatin-induced DNA Damage—A genome-wide scan for hypersensitivity to the DNA-damaging agents cisplatin and oxaliplatin (10) yielded three novel uncharacterized genes, including platinum sensitivity 2 (*PSY2*; YNL201c; Ref. 10). Interestingly *PPH3* deletion was also found to render cells hypersensitive to cisplatin treatment (10). Deletion of *PPH3* or *PSY2* was also reported to moderately increase the sensitivity of *S. cerevisiae* to methyl methanesulfonate (38). Because in mammalian cells PP4R2 is an obligatory partner for the association of PP4C and PP4R3, and Tip41 associates with PP4cs in yeast and mammals, we characterized the sensitivity of yeast lacking the *YBL046W* or *TIP41* (*YPR040W*) genes to cisplatin treatment. Diploid yeast strains were treated with cisplatin or vehicle alone, and the growth of yeast was monitored 36 h after plating onto fresh YPD agar plates. As expected from the large scale studies, deletion of *PPH3*, *PSY2*, or the polymerase ζ-associated protein *REV1*, rendered cells hypersensitive to cisplatin treatment (Fig. 3*C*). Importantly, and consistent with a role for the entire yeast PP4cs complex in cisplatin sensitivity, deletion of *YBL046W* also elicited cisplatin hypersensitivity. Interestingly, deletion of *TIP41* yielded an intermediate phenotype, exhibiting more sensitivity than a wild type strain yet less sensitivity than the *PSY2*, *PPH3*, or *YBL046W* deletants. Strains deleted for the *PPH3*-related *PPH22* or *PPZ2* phosphatases displayed cisplatin sensitivity similar to the parental strain in this screen. To control for spurious results due to secondary mutations, we repeated the experiment with a haploid deletion set and obtained identical results (Fig. 3*D*). Thus, the yeast PP4 complex containing Pph3, Ybl046w, and Psy2 plays a crucial role in viability following cisplatin-induced DNA damage. Tip41 may play a role as a modulator or facilitator perhaps by making the PP4 complex more available to substrate(s) following DNA damage treatment.

Because Psy2, Pph3, and Ybl046w interacted with Spt4 and Spt5 in the TAP tag pull-down experiments and Spt4 was implicated in the shutdown of Pol II-mediated transcription following DNA damage (possibly via dephosphorylation of Pol II Ser-5; Ref. 39), we reasoned that the involvement of the PP4cs proteins in cisplatin resistance may be effected

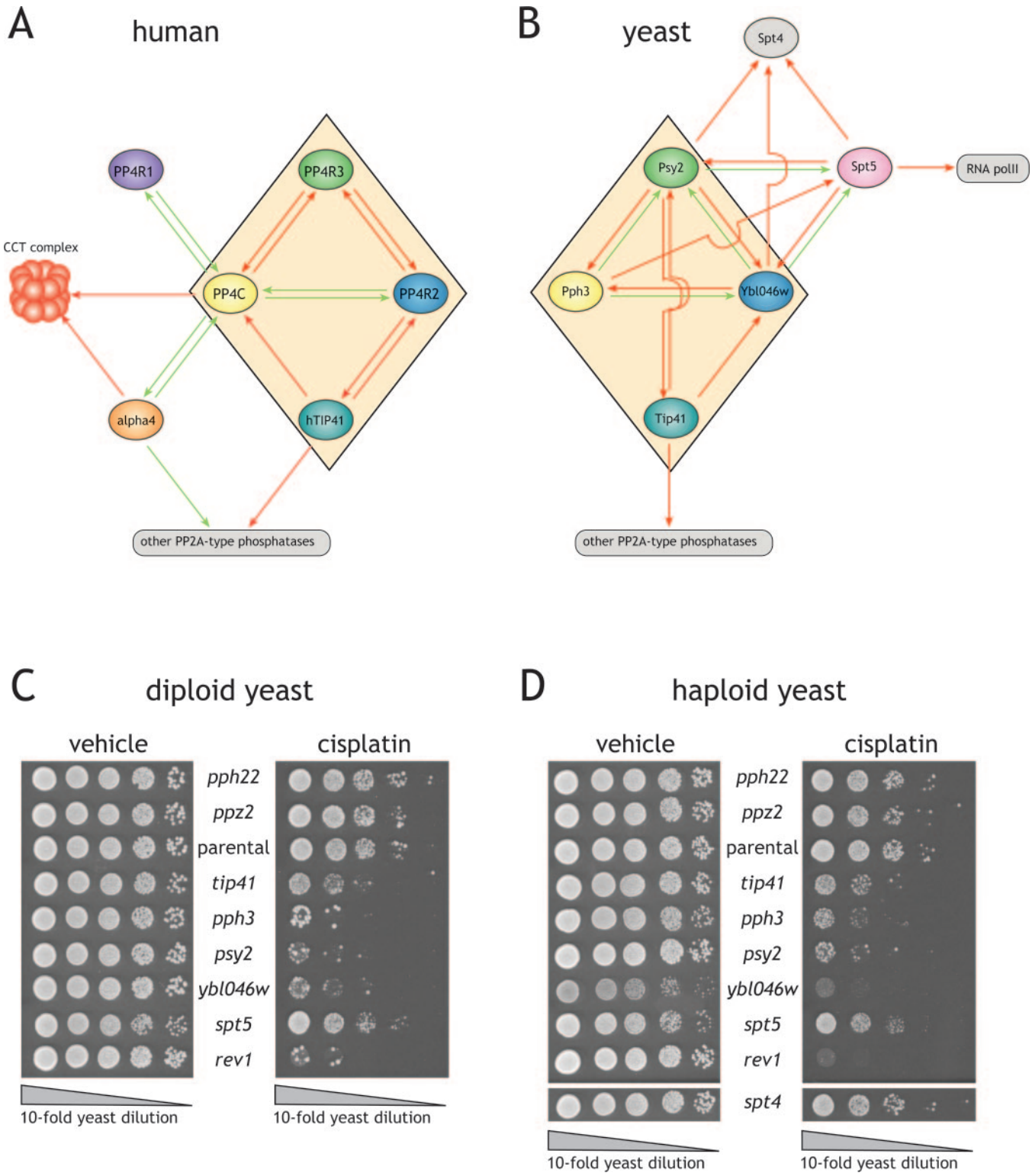

FIG. 3. **Comparison of yeast and human PP4C interaction maps and cisplatin sensitivity of individual yeast deletion strains.** *A* and *B*, schematic organization of the multiprotein complexes recovered and identified by TAP tagging and mass spectrometry. Human data are also shown in Fig. 1 and Table I; yeast data are extracted from Table II. *Arrows* denote directionality of the interaction (bait → prey) and are *color-coded* as in Fig. 1. *Colored nodes* represent proteins used as bait in the TAP tagging procedure, whereas *gray nodes* represent proteins that were not analyzed further. The *beige diamond* encompasses the PP4C·PP4R2·PP4R3·hTip41 complex conserved from yeast to mammals. *C* and *D*, cisplatin sensitivity of yeast strains harboring deletions for PP4cs complex components. Diploid (*C*) or haploid (*D*) *S. cerevisiae*

through *SPT4* and *SPT5*. Therefore, homozygous diploid *SPT5* deletant and haploid *SPT4* and *SPT5* deletion strains were tested for cisplatin sensitivity. In the absence of cisplatin, both strains grew slightly slower than the parental strain. However, none of the *SPT4/5* strains exhibited significant hypersensitization to cisplatin (Fig. 3, *C* and *D*). Thus, *SPT4* and *SPT5* are not likely to be key mediators of the cisplatin sensitivity caused by PP4cs deletion.

Psy2 Interacts with Rad53—In an attempt to elucidate how PP4cs and Tip41 are connected to the DNA damage repair machinery, we turned to a yeast two-hybrid strategy. Psy2 was previously reported to interact with Rad53 in the yeast two-hybrid assay (Rad53 was used as bait; Ref. 13). We attempted to verify this interaction using the reverse configuration with Rad53 cloned into a prey vector and Psy2 expressed from a bait vector. In addition, we tested pairwise interactions among all of the components of our yeast PP4 complex and explored putative interactions with other components of the DNA damage machinery. A total of 31 nonredundant prey-containing yeast strains were mated in duplicate to strains expressing Psy2, Ybl046w, Pph3, Tip41, and Rad53 from the bait vector. Although a previous study utilized Rad53 as bait, our own bait strains harboring Rad53 mated inefficiently, and two-hybrid interactions could not be tested for this strain. The other bait strains were tested in a 96-well format, and the growth of colonies on media lacking histidine was monitored. By plating the yeast on selection media containing varying amounts of 3-aminotriazole (a stoichiometric inhibitor of His3p activity), background levels could be efficiently controlled such that growth of negative controls (*e.g.* vector alone) served as a base line to score positives. As previously reported, bidirectional interactions were detected between Psy2 and Ybl046w (Fig. 4, *A* and *B*). In addition, Tip41 (bait) interacted with Pph3 (prey), Pph21, Pph22 (Fig. 4*A*), Sit4, and Ppg1 (not shown). We also detected a previously unreported bidirectional interaction between Pph3 and Ybl046w. Consistent with our TAP tag data, Psy2 strongly interacted with Spt4 and Spt5 in the two-hybrid assay. Finally a strong signal was also observed between Psy2 (bait) and Rad53 (prey). No signal was detected for Rad53 with any of the other baits tested. Additionally no signal was detected between any of the baits tested and strains containing prey vectors expressing other proteins involved in DNA damage (not shown). These data suggest that the yeast PP4cs complex is connected to the DNA damage machinery via an interaction between Psy2 (PP4R3) and Rad53.

PP4R3 Is a Functional Homolog of Psy2—To determine whether the yeast and human PP4cs are functionally equivalent in the cisplatin sensitivity assay, we reintroduced a FLAG-tagged galactose-inducible Psy2 or mammalian PP4R3 (or vector alone) into the *psy2*Δ diploid strain. We then performed cisplatin sensitivity assays as above. As expected, the *psy2*Δ strain (transformed with vector alone) was much more sensitive to cisplatin treatment than the parental strain (transformed with vector alone; Fig. 5*A*), although the magnitude of this effect was less pronounced on the synthetic defined media used for this assay than on YPD media as used in Fig. 4. *psy2*Δ strains transformed with FLAG-Psy2 (two independent transformants tested) exhibited a level of cisplatin sensitivity similar to the parental strain (Fig. 5*A*). Strikingly expression of FLAG-tagged mammalian PP4R3 also reverted the cisplatin hypersensitivity of a *psy2*Δ strain, indicating that Psy2 and PP4R3 are functionally equivalent in mediating resistance to cisplatin.

To determine whether human PP4R3 can establish the same two-hybrid contacts with the yeast prey proteins as Psy2, we mated a yeast bait strain expressing human PP4R3 to our prey array. Although we did not detect interactions with Ybl046w, Spt4, or Spt5, PP4R3 strongly interacted with yeast Rad53 (this was, in fact, the only interaction we detected; Fig. 5*B*). It thus appears that an interaction between PP4R3/Psy2 and the DNA damage machinery has been evolutionarily conserved.

Cisplatin Hypersensitivity of PP4R3 Mutants in Higher Eukaryotes—To investigate whether a reduction in PP4R3 activity renders a multicellular organism hypersensitive to cisplatin, we assayed animals harboring mutations in the *Drosophila* falafel (*flfl*) gene, which encodes the fly homolog of the PP4R3/Psy2 protein (Fig. 1*C*). Two ethyl methanesulfonate-induced mutant alleles, $flfl^2$ and $flfl^3$ (see "Experimental Procedures"), were identified in a reversion assay for an enhancer and promoter-mediated *flfl* gain-of-function phenotype.[2] Although flies homozygous for either mutation ($flfl^2/flfl^2$ or $flfl^3/flfl^3$) were inviable, 30% of animals possessing the heteroallelic combination $flfl^2/flfl^3$ reached adulthood and displayed a statistically significant reduction in size as compared with their wild type counterparts (weight reduction of ~23% in females and ~12% in males).

Mutant first instar $flfl^2/flfl^3$ larvae were placed onto standard fly food supplemented with increasing concentrations of cisplatin (see "Experimental Procedures"), and emerging adult flies were counted 3 days after eclosion. (The survival of mutant $flfl^2/flfl^3$ animals is compromised even in the absence of cisplatin, so these data were normalized to the survival of *flfl* mutants in the absence of the drug.) Survival curves for $flfl^2/flfl^3$ mutants and control animals grown on increasing

[2] M. Zarske and E. Hafen, manuscript in preparation.

deletion mutants were grown to OD ~ 0.4 and then treated with 1 mM cisplatin (or DMSO vehicle alone) for 4 h. Serial 10-fold dilutions were plated onto YPD, and growth was monitored 36 h post-treatment. Pph22 is a yeast homolog of the PP2A catalytic subunit, whereas Ppz2 is a homolog of the human PP1 catalytic subunit. *rev1*Δ was used here as a positive control.

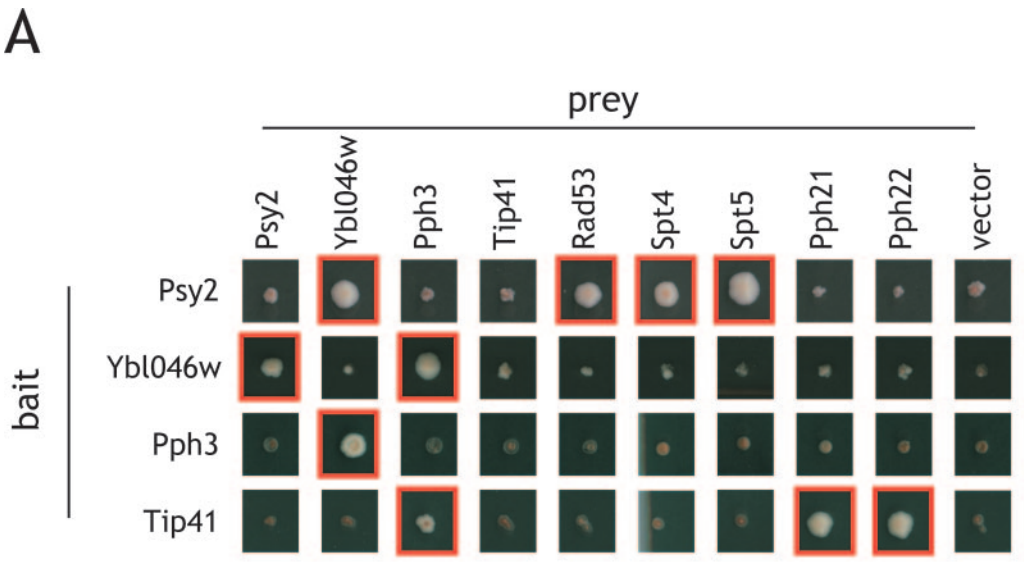

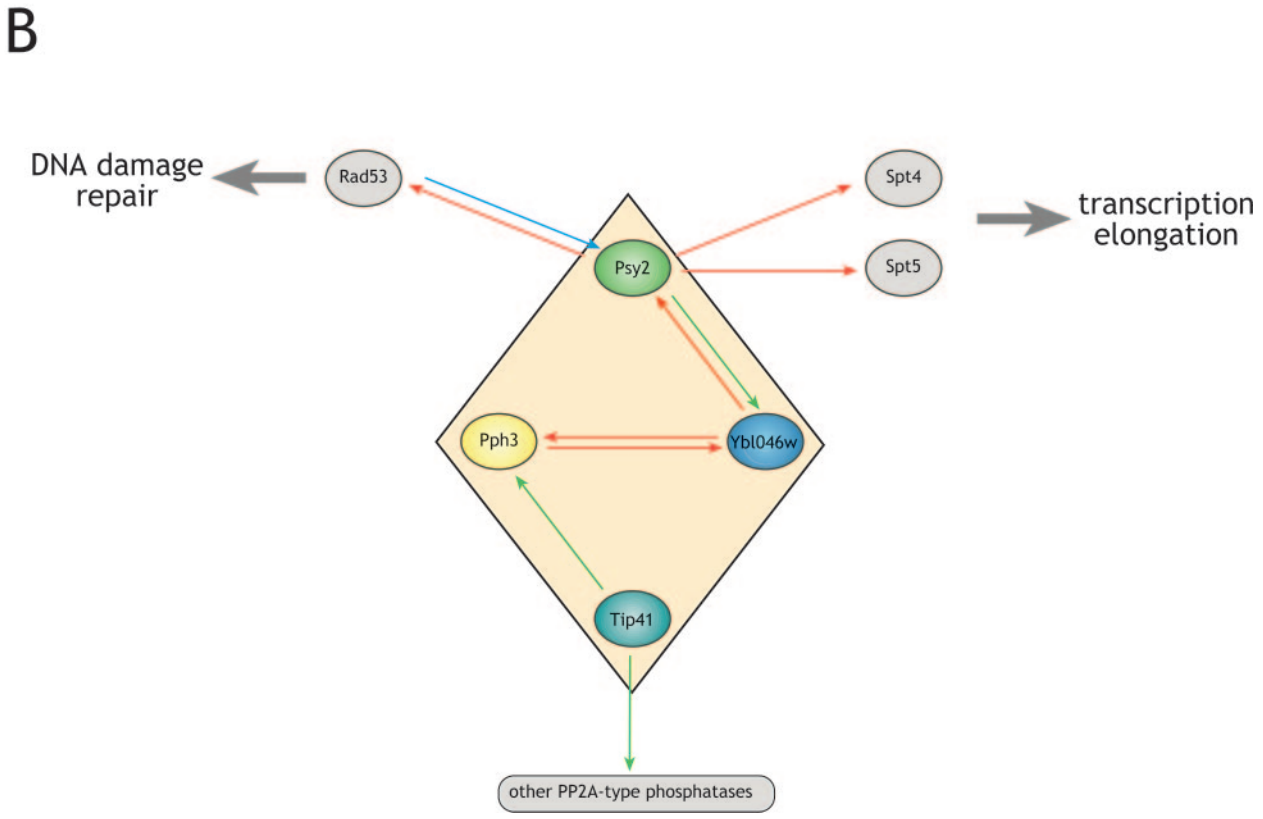

FIG. 4. **Psy2p interacts with Rad53p.** Coding sequences for Psy2p, Ybl046w, Pph3p, and Tip41p were cloned into the yeast two-hybrid bait vector pOBD-2, and the constructs were transfected into the pJ69-4a strain. A miniarray of "prey" in pOAD/pJ69-4α, extracted from a larger collection described previously (13), was supplemented with a collection of cDNAs coding for Psy2, Ybl046w, Pph3, Tip41, and Rad53 in pOAD/pJ69-4α and generated in parallel to the bait. The final prey array consisted of the following proteins: Spt4, Rad6, Rev7, Mrc1, Ybl046w,

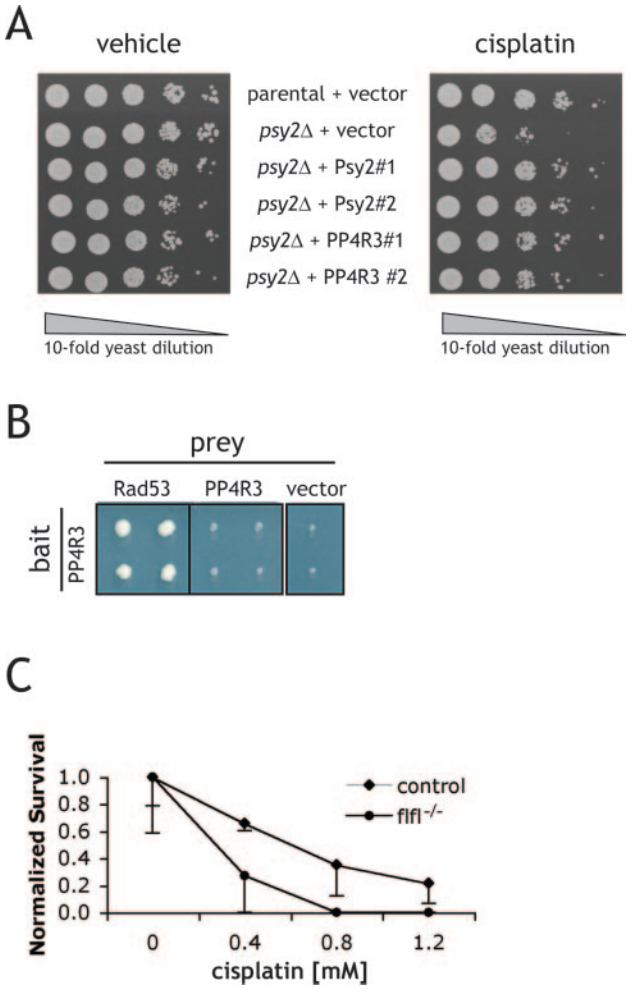

FIG. 5. **PP4R3 from higher eukaryotes is involved in cisplatin sensitivity.** *A*, mammalian PP4R3 functionally replaces *PSY2* in the cisplatin sensitivity assay. Yeast Psy2 or mammalian PP4R3 cDNAs were cloned into the galactose-inducible pESC-ura vector and transformed into the diploid yeast strain lacking *PSY2*. Individual clones were selected. Expression of the recombinant cDNAs was driven through growth on galactose for 8 h prior to cisplatin treatment (4 h). A serial 10-fold dilution series was plated onto minimal medium lacking uracil but containing galactose to maintain expression. Growth was monitored 48 h post-treatment. *B*, mammalian PP4R3 interacts with yeast Rad53. A yeast two-hybrid assay using human PP4R3 as bait was performed as in Fig. 5 in duplicate. *C*, flies lacking functional PP4R3 (*flfl*) are hypersensitive to cisplatin. Survival of *flfl* heterozygous (control, MKRS/$flfl^2$, or MKRS/$flfl^3$) and $flfl^2/flfl^3$ heteroallelic mutant female flies following cisplatin treatment. Numbers of surviving flies at various concentrations of cisplatin were normalized to the numbers of untreated animals. Similar results were obtained with male flies. Experiments were performed in triplicate at all concentrations with ~100 flies per concentration.

concentrations of cisplatin are shown in Fig. 5*C*. Female $flfl^2/flfl^3$ mutant flies displayed reduced survival at 0.4 μM cisplatin compared with wild type flies (Fig. 5*C*). No $flfl^2/flfl^3$ individuals survived when exposed to 0.8 or 1.2 μM cisplatin, whereas some wild type animals emerged (identical results were observed with male *flfl* mutant animals; data not shown). These results suggest that falafel (PP4reg3) function in higher eukaryotes is required for resistance to cisplatin treatment and provide further evidence for a critical and evolutionarily conserved role of this PP4C-interacting partner in the response to DNA damage.

DISCUSSION

Here, using an iterative TAP tagging/mass spectrometry approach, we report that the mammalian PP4 catalytic subunit is a component of several different mutually exclusive subcomplexes: one containing PP4R1, another containing alpha4 and the TRiC/CCT complex, and a third (PP4cs) containing PP4R2 and a novel protein that we termed PP4R3. The PP4cs complex is evolutionarily conserved and in yeast is composed of the Pph3, Ybl046w, and Psy2 proteins. The conservation in *S. cerevisiae* suggested a role for PP4cs in resistance to cytotoxic agents: genome-wide screens of the yeast deletion collection with the DNA-damaging agents cisplatin, oxaliplatin, mitomycin C, and methyl methanesulfate have highlighted the importance of both *PPH3* and *PSY2* in survival following exposure to these agents (10, 38). We demonstrated that yeast strains deleted for *YBL046W* (PP4R2) are hypersensitive to cisplatin to the same extent as strains deleted for either *PPH3* or *PSY2*. The mammalian ortholog of Psy2, PP4R3, could substitute for the yeast protein in cisplatin sensitivity assays, suggesting that the mammalian complex plays a similar role. Furthermore in *Drosophila*, mutation of the falafel gene, the ortholog of Psy2, led to increased cisplatin sensitivity.

How might the PP4C·PP4R2·PP4R3 complex be linked to the DNA damage response? A previous yeast two-hybrid screen for Rad53-interacting partners yielded Psy2 (13). We confirmed this observation and demonstrated that the interaction is independent of Rad53 kinase activity (data not shown). Rad53 (or CHK2 in humans) is a critical component in a DNA damage checkpoint response conserved from yeast to humans (human ortholog CHK2; Refs. 40 and 41). We were not able to detect Rad53-Psy2 or human CHK2-PP4R3 interactions by pull-down assay, suggesting that these interactions are transient or easily disrupted through our purification protocol or that the interactions may be substoichiometric.

Rad18, Rrd1, Rad10, Rad2, Pho85, Ppg1, Luc7, Pph3, Rrd2, Tip41, Pph22, Pph21, Ynr069c, Ahc1, Hol1, Psy2, Rad53, Rev1, Rad1, Spt5, Rad26, Rad9, Rev3, Mec1, Sit4, and Mrp144. Bait and prey strains were mated, and growth on selective medium (lacking histidine and containing various amounts of 3-aminotriazole) was monitored. *A*, representative results for each mating. Positive results are *framed* in *red*. *B*, summary of the interactions detected by the yeast two-hybrid method in this and other studies. Proteins used as bait are denoted by *colored nodes*. *Red arrows* indicate novel interactions reported for the first time in this study; *green arrows* indicate interactions detected in this study as in previous reports; and the *blue arrow* represents an interaction reported in the literature but not tested here.

Other links between PP4cs and DNA damage also exist. Yeast PP4cs associates with Spt4 and Spt5, transcription elongation factor proteins linked to DNA damage-induced Pol II dephosphorylation at Ser-5, and subsequent transcriptional shutdown (39). However, deletion of Spt4 or Spt5 did not result in hypersensitivity to cisplatin, indicating that the PP4cs-Spt4-Spt5 interaction is not sufficient to explain the cisplatin sensitivity phenotype.

Psy2 was also reported previously to genetically and physically interact with Wss1 and Tof1, two proteins presumed to play a role in the stabilization of stalled replication forks (42). In human cells, additional links between PP4C and/or the PP4cs complex and cisplatin-induced DNA damage may exist. For instance, cisplatin-induced NF-κB activation appears to be mediated, at least in part, by PP4C-mediated dephosphorylation of NF-κB p65 at Thr-435 (43). The precise contribution of each of these pathways to the cisplatin hypersensitivity phenotype of the PP4cs deletants remains to be assessed.

Cisplatin and related platinum compounds such as carboplatin are effective against many types of solid tumors, including cervical, ovarian, head-and-neck, and non-small cell lung cancers (for a review, see Ref. 44). Cisplatin analogs have also proven particularly effective against testicular cancer for which the overall cure rate exceeds 90% (for a review, see Ref. 12). However, intrinsic or acquired resistance to cisplatin analogs is frequently encountered, significantly limiting the application of this class of drugs (12). Resistance may be attributed to several factors, including decreased drug accumulation, increased cellular detoxification, enhanced DNA repair, tolerance to platinum-induced DNA damage, and alterations in signal transduction pathways (11). Cisplatin resistance is thus a major hurdle in cancer therapies, and a primary goal in designing new platinum-based anticancer agents has been to circumvent this problem (45).

The sensitization to cisplatin of *S. cerevisiae* deleted for any of the PP4cs members suggests that inactivation of the human PP4cs components during cisplatin treatment may sensitize cisplatin-resistant tumor cells to the drug. In support of this possibility, two different cell lines selected for cisplatin resistance through long term cisplatin treatment demonstrated a striking reversal to a sensitive phenotype when co-treated with low doses of demethylcantharidin or okadaic acid, two PP2A inhibitors (46, 47). PP4C is also sensitive to these compounds (48) and was likely inhibited in these studies. Novel platinum-based compounds comprised of two moieties, the platinum group and demethylcantharidin, elicited sensitivity of these cisplatin-resistant cell lines only when the compounds exhibited activity toward PP2A (46, 47). Based on the shared sensitivity of PP2AC and PP4C to cantharidin-based compounds, PP4C is also likely targeted by these compounds. A drug that targets the assembly of PP4cs, perhaps by preventing PP4R2 from binding to PP4C or PP4R3, could thus potentially synergize with cisplatin while having fewer side effects than drugs inhibiting all PP2A-type subunits.

Finally a different type of anticancer compound, rapamycin, was also demonstrated to enhance cisplatin sensitivity in cell and animal models (*e.g.* Ref. 49). Rapamycin actions are conserved from yeast to humans and appear to involve modulation of PP2A-type phosphatase activity through Tap42 (alpha4) and Tip41 (at least in yeast). Rapamycin analogs are used in the clinic to prevent graft rejection and as anticancer agents (for reviews, see Refs. 50 and 51). Recently the synergy between cisplatin and rapamycin was demonstrated to be attributable to changes in the levels of the p21 protein because of a modest general decrease in translation brought about by rapamycin (52). Whether PP4cs plays a role in the control of translation and the regulation of p21 levels remains to be investigated.

Further delineation of the interacting partners and supramolecular architecture of the PP2A-type phosphatases should greatly assist us in deciphering the roles that each of these important proteins plays in various cellular processes. Given that these enzymes play critical roles in DNA repair and tumor promotion (4), a more intimate understanding of their regulation and function should provide us with greater treatment options for various types of cancers.

Acknowledgments—We thank Drs. K. T. Arndt, K. L. Gould, H. Imataka, M. Marelli, and S. Morino for the kind gifts of reagents and Drs. R. Bonneau, M. N. Hall, H. Stocker, B. Wadzinski, and members of the Aebersold, Aitchison, and Galitski laboratories for helpful discussions. We thank Drs. M. Miron, S. Prinz, J. A. Ranish, G. Thomas, and B. Wollscheid for critical review of the manuscript.

* This work was supported in part by federal funds from the NHLBI, National Institutes of Health, under Contract Number N01-HV-28179 (to R. A.) and from National Center for Research Resources Grant P41 RR11823 (to S. F.). The costs of publication of this article were defrayed in part by the payment of page charges. This article must therefore be hereby marked "*advertisement*" in accordance with 18 U.S.C. Section 1734 solely to indicate this fact.

S The on-line version of this article (available at http://www.mcponline.org) contains supplemental material.

§ Supported by a postdoctoral fellowship from the Canadian Institutes of Health Research. To whom correspondence should be addressed. Tel.: 206-732-1393; Fax: 206-732-1299; E-mail: agingras@systemsbiology.org.

** An investigator of the Howard Hughes Medical Institute.

REFERENCES

1. Barford, D., Das, A. K., and Egloff, M. P. (1998) The structure and mechanism of protein phosphatases: insights into catalysis and regulation. *Annu. Rev. Biophys. Biomol. Struct.* **27,** 133–164
2. Andreeva, A. V., and Kutuzov, M. A. (2001) PPP family of protein Ser/Thr phosphatases: two distinct branches? *Mol. Biol. Evol.* **18,** 448–452
3. Cohen, P. T. (1997) Novel protein serine/threonine phosphatases: variety is the spice of life. *Trends Biochem. Sci.* **22,** 245–251
4. Janssens, V., Goris, J., and Van Hoof, C. (2005) PP2A: the expected tumor suppressor. *Curr. Opin. Genet. Dev.* **15,** 34–41
5. Sontag, E. (2001) Protein phosphatase 2A: the Trojan Horse of cellular signaling. Cell. Signal. **13,** 7–16
6. Kloeker, S., and Wadzinski, B. E. (1999) Purification and identification of a

novel subunit of protein serine/threonine phosphatase 4. *J. Biol. Chem.* **274,** 5339–5347
7. Hastie, C. J., Carnegie, G. K., Morrice, N., and Cohen, P. T. (2000) A novel 50 kDa protein forms complexes with protein phosphatase 4 and is located at centrosomal microtubule organizing centres. *Biochem. J.* **347,** 845–855
8. Carnegie, G. K., Sleeman, J. E., Morrice, N., Hastie, C. J., Peggie, M. W., Philp, A., Lamond, A. I., and Cohen, P. T. (2003) Protein phosphatase 4 interacts with the Survival of Motor Neurons complex and enhances the temporal localisation of snRNPs. *J. Cell Sci.* **116,** 1905–1913
9. Zhang, X., Ozawa, Y., Lee, H., Wen, Y. D., Tan, T. H., Wadzinski, B. E., and Seto, E. (2005) Histone deacetylase 3 (HDAC3) activity is regulated by interaction with protein serine/threonine phosphatase 4. *Genes Dev.* **19,** 827–839
10. Wu, H. I., Brown, J. A., Dorie, M. J., Lazzeroni, L., and Brown, J. M. (2004) Genome-wide identification of genes conferring resistance to the anticancer agents cisplatin, oxaliplatin, and mitomycin C. *Cancer Res*. **64,** 3940–3948
11. Siddik, Z. H. (2003) Cisplatin: mode of cytotoxic action and molecular basis of resistance. *Oncogene* **22,** 7265–7279
12. Wang, D., and Lippard, S. J. (2005) Cellular processing of platinum anticancer drugs. *Nat. Rev. Drug Discov.* **4,** 307–320
13. Uetz, P., Giot, L., Cagney, G., Mansfield, T. A., Judson, R. S., Knight, J. R., Lockshon, D., Narayan, V., Srinivasan, M., Pochart, P., Qureshi-Emili, A., Li Y., Godwin, B., Conover, D., Kalbfleisch, T., Vijayadamodar, G., Yang, M., Johnston, M., Fields, S., and Rothberg, J. M. (2000) A comprehensive analysis of protein-protein interactions in Saccharomyces cerevisiae. *Nature* **403,** 623–627
14. Hazbun, T. R., and Miller, J. P. (2005) Genome-wide analysis of protein-protein interactions by a two-hybrid assay, in *Protein-Protein Interactions, a Molecular Cloning Manual*, Cold Spring Harbor Press, Cold Spring Harbor, NY, in press
15. Tasto, J. J., Carnahan, R. H., McDonald, W. H., and Gould, K. L. (2001) Vectors and gene targeting modules for tandem affinity purification in Schizosaccharomyces pombe. *Yeast* **18,** 657–662
16. Rigaut, G., Shevchenko, A., Rutz, B., Wilm, M., Mann, M., and Seraphin, B. (1999) A generic protein purification method for protein complex characterization and proteome exploration. *Nat. Biotechnol.* **17,** 1030–1032
17. Pedrioli, P. G., Eng, J. K., Hubley, R., Vogelzang, M., Deutsch, E. W., Raught, B., Pratt, B., Nilsson, E., Angeletti, R. H., Apweiler, R., Cheung, K., Costello, C. E., Hermjakob, H., Huang, S., Julian, R. K., Kapp, E., McComb, M. E., Oliver, S. G., Omenn, G., Paton, N. W., Simpson, R., Smith, R., Taylor, C. F., Zhu, W., and Aebersold, R. (2004) A common open representation of mass spectrometry data and its application to proteomics research. *Nat. Biotechnol.* **22,** 1459–1466
18. Han, D. K., Eng, J., Zhou, H., and Aebersold, R. (2001) Quantitative profiling of differentiation-induced microsomal proteins using isotope-coded affinity tags and mass spectrometry. *Nat. Biotechnol.* **19,** 946–951
19. Keller, A., Nesvizhskii, A. I., Kolker, E., and Aebersold, R. (2002) Empirical statistical model to estimate the accuracy of peptide identifications made by MS/MS and database search. *Anal. Chem.* **74,** 5383–5392
20. Nesvizhskii, A. I., Keller, A., Kolker, E., and Aebersold, R. (2003) A statistical model for identifying proteins by tandem mass spectrometry. *Anal. Chem.* **75,** 4646–4658
21. Gingras, A. C., Aebersold, R., and Raught, B. (2005) Advances in protein complex analysis using mass spectrometry. *J. Physiol.* **563,** 11–21
22. Puig, O., Caspary, F., Rigaut, G., Rutz, B., Bouveret, E., Bragado-Nilsson, E., Wilm, M., and Seraphin, B. (2001) The tandem affinity purification (TAP) method: a general procedure of protein complex purification. Methods **24,** 218–229
23. Gomez-Puertas, P., Martin-Benito, J., Carrascosa, J. L., Willison, K. R., and Valpuesta, J. M. (2004) The substrate recognition mechanisms in chaperonins. *J. Mol. Recognit.* **17,** 85–94
24. Chen, J., Peterson, R. T., and Schreiber, S. L. (1998) Alpha4 associates with protein phosphatases 2A, 4, and 6. *Biochem. Biophys. Res. Commun.* **247,** 827–832
25. Duvel, K., and Broach, J. R. (2004) The role of phosphatases in TOR signaling in yeast. *Curr. Top. Microbiol. Immunol.* **279,** 19–38
26. Di Como, C. J., and Arndt, K. T. (1996) Nutrients, via the Tor proteins, stimulate the association of Tap42 with type 2A phosphatases. *Genes Dev.* **10,** 1904–1916
27. Murata, K., Wu, J., and Brautigan, D. L. (1997) B cell receptor-associated protein alpha4 displays rapamycin-sensitive binding directly to the catalytic subunit of protein phosphatase 2A. *Proc. Natl. Acad. Sci. U. S. A.* **94,** 10624–10629
28. Nanahoshi, M., Nishiuma, T., Tsujishita, Y., Hara, K., Inui, S., Sakaguchi, N., and Yonezawa, K. (1998) Regulation of protein phosphatase 2A catalytic activity by alpha4 protein and its yeast homolog Tap42. *Biochem. Biophys. Res. Commun*. **251,** 520–526
29. Ho, Y., Gruhler, A., Heilbut, A., Bader, G. D., Moore, L., Adams, S. L., Millar, A., Taylor, P., Bennett, K., Boutilier, K., Yang, L., Wolting, C., Donaldson, I., Schandorff, S., Shewnarane, J., Vo, M., Taggart, J., Goudreault, M., Muskat, B., Alfarano, C., Dewar, D., Lin, Z., Michalickova, K., Willems, A. R., Sassi, H., Nielsen, P. A., Rasmussen, K. J., Andersen, J. R., Johansen, L. E., Hansen, L. H., Jespersen, H., Podtelejnikov, A., Nielsen, E., Crawford, J., Poulsen, V., Sorensen, B. D., Matthiesen, J., Hendrickson, R. C., Gleeson, F., Pawson, T., Moran, M. F., Durocher, D., Mann, M., Hogue, C. W., Figeys, D., and Tyers, M. (2002) Systematic identification of protein complexes in Saccharomyces cerevisiae by mass spectrometry. *Nature* **415,** 180–183
30. Kelley, L. A., MacCallum, R. M., and Sternberg, M. J. (2000) Enhanced genome annotation using structural profiles in the program 3D-PSSM. *J. Mol. Biol.* **299,** 499–520
31. Kittler, R., Putz, G., Pelletier, L., Poser, I., Heninger, A. K., Drechsel, D., Fischer, S., Konstantinova, I., Habermann, B., Grabner, H., Yaspo, M. L., Himmelbauer, H., Korn, B., Neugebauer, K., Pisabarro, M. T., and Buchholz, F. (2004) An endoribonuclease-prepared siRNA screen in human cells identifies genes essential for cell division. *Nature* **432,** 1036–1040
32. Zarske, M., and Hafen, E. (2003) Falafel, a novel EVH1 domain protein involved in Rac mediated epithelial morphogenesis, in *44th Annual Drosophila Research Conference*, *Chicago, March 5–9, 2003*, The Genetics Society of America, Bethesda, MD
33. Jacinto, E., Guo, B., Arndt, K. T., Schmelzle, T., and Hall, M. N. (2001) TIP41 interacts with TAP42 and negatively regulates the TOR signaling pathway. *Mol. Cell* **8,** 1017–1026
34. Kloeker, S., Bryant, J. C., Strack, S., Colbran, R. J., and Wadzinski, B. E. (1997) Carboxymethylation of nuclear protein serine/threonine phosphatase X. *Biochem. J.* **327,** 481–486
35. Ito, T., Chiba, T., Ozawa, R., Yoshida, M., Hattori, M., and Sakaki, Y. (2001) A comprehensive two-hybrid analysis to explore the yeast protein interactome. *Proc. Natl. Acad. Sci. U. S. A.* **98,** 4569–4574
36. Li, X., and Virshup, D. M. (2002) Two conserved domains in regulatory B subunits mediate binding to the A subunit of protein phosphatase 2A. *Eur. J. Biochem.* **269,** 546–552
37. Gavin, A. C. Bosche, M., Krause, R., Grandi, P., Marzioch, M., Bauer, A., Schultz, J., Rick, J. M., Michon, A. M., Cruciat, C. M., Remor, M., Hofert, C., Schelder, M., Brajenovic, M., Ruffner, H., Merino, A., Klein, K., Hudak, M., Dickson, D., Rudi, T., Gnau, V., Bauch, A., Bastuck, S., Huhse, B., Leutwein, C., Heurtier, M. A., Copley, R. R., Edelmann, A., Querfurth, E., Rybin, V., Drewes, G., Raida, M., Bouwmeester, T., Bork, P., Seraphin, B., Kuster, B., Neubauer, G., and Superti-Furga, G. (2002) Functional organization of the yeast proteome by systematic analysis of protein complexes. *Nature* **415,** 141–147
38. Hanway, D., Chin, J. K., Xia, G., Oshiro, G., Winzeler, E. A., and Romesberg, F. E. (2002) Previously uncharacterized genes in the UV- and MMS-induced DNA damage response in yeast. *Proc. Natl. Acad. Sci. U. S. A.* **99,** 10605–10610
39. Jansen, L. E., Belo, A. I., Hulsker, R., and Brouwer, J. (2002) Transcription elongation factor Spt4 mediates loss of phosphorylated RNA polymerase II transcription in response to DNA damage. *Nucleic Acids Res.* **30,** 3532–3539
40. Motoyama, N., and Naka, K. (2004) DNA damage tumor suppressor genes and genomic instability. *Curr. Opin. Genet. Dev.* **14,** 11–16
41. Quivy, J. P., and Almouzni, G. (2003) Rad53: a controller ensuring the fine-tuning of histone levels. *Cell* **115,** 508–510
42. O'Neill, B. M., Hanway, D., Winzeler, E. A., and Romesberg, F. E. (2004) Coordinated functions of WSS1, PSY2 and TOF1 in the DNA damage response. *Nucleic Acids Res.* **32,** 6519–6530
43. Yeh, P. Y., Yeh, K. H., Chuang, S. E., Song, Y. C., and Cheng, A. L. (2004) Suppression of MEK/ERK signaling pathway enhances cisplatin-induced NF-κB activation by protein phosphatase 4-mediated NF-κB p65 Thr dephosphorylation. *J. Biol. Chem.* **279,** 26143–26148

44. Jamieson, E.R., and Lippard, S.J. (1999) Structure, recognition, and processing of cisplatin-DNA adducts. *Chem. Rev.* **99,** 2467–2498
45. Ho, Y. P., Au-Yeung, S. C., and To, K. K. (2003) Platinum-based anticancer agents: innovative design strategies and biological perspectives. *Med. Res. Rev.* **23,** 633–655
46. To, K. K., Ho, Y. P., and Au-Yeung, S. C. (2005) Synergistic interaction between platinum-based antitumor agents and demethylcantharidin. *Cancer Lett.* **223,** 227–237
47. To, K. K., Wang, X., Yu, C. W., Ho, Y. P., and Au-Yeung, S. C. (2004) Protein phosphatase 2A inhibition and circumvention of cisplatin cross-resistance by novel TCM-platinum anticancer agents containing demethylcantharidin. *Bioorg. Med. Chem.* **12,** 4565–4573
48. Hastie, C. J., and Cohen, P. T. (1998) Purification of protein phosphatase 4 catalytic subunit: inhibition by the antitumour drug fostriecin and other tumour suppressors and promoters. *FEBS Lett.* **431,** 357–361
49. Shi, Y., Frankel, A., Radvanyi, L. G., Penn, L. Z., Miller, R. G., and Mills, G. B. (1995) Rapamycin enhances apoptosis and increases sensitivity to cisplatin in vitro. *Cancer Res.* **55,** 1982–1988
50. Hay, N., and Sonenberg, N. (2004) Upstream and downstream of mTOR. *Genes Dev.* **18,** 1926–1945
51. Vignot, S., Faivre, S., Aguirre, D., and Raymond, E. (2005) mTOR-targeted therapy of cancer with rapamycin derivatives. *Ann. Oncol.* **16,** 525–537
52. Beuvink, I., Boulay, A., Fumagalli, S., Zilbermann, F., Ruetz, S., O'Reilly, T., Natt, F., Hall, J., Lane, H. A., and Thomas, G. (2005) The mTOR inhibitor RAD001 sensitizes tumor cells to DNA-damaged induced apoptosis through inhibition of p21 translation. *Cell* **120,** 747–759